AD_____

Award Number: W81XWH-05-1-0396

TITLE: Angiogenic Signaling in Living Breast Tumor Models

PRINCIPAL INVESTIGATOR: Edward Brown, M.D.

CONTRACTING ORGANIZATION: University of Rochester
Rochester, NY 14627-0140

REPORT DATE: June 2007

TYPE OF REPORT: Annual

PREPARED FOR: U.S. Army Medical Research and Materiel Command
Fort Detrick, Maryland 21702-5012

DISTRIBUTION STATEMENT: Approved for Public Release;
Distribution Unlimited

REPORT DOCUMENTATION PAGE

Form Approved
OMB No. 0704-0188

1. REPORT DATE *(DD-MM-YYYY)*	**2. REPORT TYPE**	**3. DATES COVERED** *(From - To)*
01-06-2007	Annual	1 Jun 2006 – 31 May 2007

4. TITLE AND SUBTITLE

Angiogenic Signaling in Living Breast Tumor Models

5a. CONTRACT NUMBER

5b. GRANT NUMBER
W81XWH-05-1-0396

5c. PROGRAM ELEMENT NUMBER

6. AUTHOR(S)

Edward Brown, M.D.

E-Mail: edward_brown@urmc.rochester.edu

5d. PROJECT NUMBER

5e. TASK NUMBER

5f. WORK UNIT NUMBER

7. PERFORMING ORGANIZATION NAME(S) AND ADDRESS(ES)

University of Rochester
Rochester, NY 14627-0140

8. PERFORMING ORGANIZATION REPORT NUMBER

9. SPONSORING / MONITORING AGENCY NAME(S) AND ADDRESS(ES)
U.S. Army Medical Research and Materiel Command
Fort Detrick, Maryland 21702-5012

10. SPONSOR/MONITOR'S ACRONYM(S)

11. SPONSOR/MONITOR'S REPORT NUMBER(S)

12. DISTRIBUTION / AVAILABILITY STATEMENT
Approved for Public Release; Distribution Unlimited

13. SUPPLEMENTARY NOTES

14. ABSTRACT

In this grant we propose to elucidate the signaling pathway that translates VEGFR activation into elevated vessel permeability, in endothelial cells within living breast tumor models. The working hypothesis is that the signaling pathway involved is a constitutively active form of the pathway shown for healthy mesenteric microvessels. Progress to date includes the training of personnel in the laboratory, the completion of instrumentation development for a novel method for the measurement of convective flow in tumors in vivo and extensive analysis of its capabilities, extensive investigation of breast tumor exctracellular matrix using second harmonic generation, extensive analysis of the abilities of a novel permeability measurement technique and numerous preliminary experiments to establish methodology for tasks to commence in upcoming years.

15. SUBJECT TERMS
Angiogenesis, microscopy, signaling, VEGF, permeability

16. SECURITY CLASSIFICATION OF:			**17. LIMITATION OF ABSTRACT**	**18. NUMBER OF PAGES**	**19a. NAME OF RESPONSIBLE PERSON**
a. REPORT	**b. ABSTRACT**	**c. THIS PAGE**			USAMRMC
U	U	U	UU	28	**19b. TELEPHONE NUMBER** *(include area code)*

Standard Form 298 (Rev. 8-98)
Prescribed by ANSI Std. Z39.18

Table of Contents

Introduction.

Current anti-angiogenic therapies focus on the earliest steps in the angiogenic signaling cascades and try to prevent angiogenic molecules (i.e. VEGF, Ang-1, TGF-α) from reaching endothelial cells or try to prevent activation of their endothelial cell (EC) receptors. However, the study of downstream steps, within tumor ECs, as an avenue for treatment has been neglected. Furthermore, due to a lack of appropriate *in vivo* imaging and measurement tools, these EC signaling cascades have been explored almost exclusively in thin preparations of healthy vessels (i.e. vessels in the easily accessible, 25 micron mesenteric membrane) or in endothelial cells in a dish, and the signaling machinery that is delineated varies depending upon which type of healthy vessel provides the ECs. As tumor vessels are fundamentally unlike any of the healthy vessels in the body, we don't know which of the known signaling pathways are involved in *in vivo* tumor angiogenesis, *or if any of them are*. Consequently, we propose to elucidate the signaling pathway that translates VEGFR activation into elevated vessel permeability, in endothelial cells within living breast tumor models. The working hypothesis is that the signaling pathway involved is a constitutively active form of the pathway shown for healthy mesenteric microvessels. We have identified several signaling molecules that we hypothesize will play key roles in that pathway. In each case we will pharmacologically enhance or inhibit the action of a given molecule, and use advanced *in vivo* imaging techniques that we are currently developing or have previously developed to probe the resultant alterations in the VEGF/permeability relationship, with EC internal calcium dynamics as a key intermediate readout. Elucidation of this pathway is motivated by the desire to find new therapeutic targets, with which to block tumor angiogenesis and hence restrict tumor growth. Current angiogenic therapies, which favor blocking transit of an angiogenic factor to the ECs or inhibition of receptor activation, often fail because there can be several parallel pathways for angiogenic signals to travel from tumor cells to ECs, and when one is blocked, others are utilized. Signaling that occurs downstream of endothelial receptor activation may provide a signaling 'bottleneck' that several angiogenic factors utilize in common and hence may provide a uniquely powerful therapeutic target which circumvents the development of drug resistance.

Body

We are now concluding the second year of this grant, as well as the second year of my laboratory, here in the Department of Biomedical Engineering at the University of Rochester Medical Center. My laboratory now consists of myself, Kelley Madden, a Research Assistant Professor in BME, and three graduate students, Ryan Burke in BME, Kelley Sullivan (formerly Dunbar) in Physics, and Xiaoxing Han in Optics. What follows is a discussion of our progress in each of the Tasks in our original Statement of Work, starting with those tasks that were scheduled to begin earliest, and finishing with later tasks.

Progress in Task 7.

Chronologically, the earliest goals in my original Statement of Work are actually encompassed in tasks 7 and 9. In its entirety, Task 7 is:

Task 7. Determine the relative contribution of convection versus diffusion in transport of fluorescent tracer out of a tumor vessel. (Years 1 and 2)

A. Develop theory and perform *in vitro* tests of the ability of Multiphoton Fluorescence Recovery After Photobleaching (MPFRAP) to simultaneously measure diffusion and convection.

B. Determine relative contribution of convection versus diffusion in transport out of a tumor vessel during steady state conditions.

C. Determine relative contribution of convection versus diffusion in transport out of a tumor vessel after acute alteration in tumor vessel permeability.

We began Year Two with work to streamline the MPFRAP procedure by building additional control equipment and by automating data taking and analysis steps. We also verified several experimental parameters for which we had previously been substituting given/derived values. Perhaps most significantly, we determined much of the range of velocities, diffusion coefficients and signal to noise ratios over which the MP-FRAP technique is valid.

In order to reduce significant electrical noise in our first system, we designed and constructed a new control box to take over the switching mechanism previously provided by the pulse generator to toggle between bleach and monitor laser powers and select those powers with microsecond time resolution. This control box also increases the efficiency of adjusting the laser powers and aligning our Pockels Cell. To reduce measurement time and increase throughput, we automated data generation and analysis procedures using an extensive series of LabVIEW and Matlab programs to run all the equipment and to collect, graph and export data (to file), and to analyze that data and produce fits.

We have also verified several experimental parameters, including the point spread function (PSF) of our two-photon focal spot. The PSF appears in the recovery equation and links two significant experimental variables, the characteristic diffusion time and the diffusion coefficient. The theoretical value of the PSF for a properly over-filled lens is given by $w_r = 2.6\lambda/(2\pi NA)$, where λ is the wavelength of laser light and NA is the numerical aperture of the lens. At an operating wavelength of 780nm and using a lens with a numerical aperture of 0.9, the theoretical PSF is 0.358μm. Our experimental measurement of the PSF yielded a comparable 0.36μm. This work has ensured that our system is functioning as expected.

We have recently resumed testing of our newly reconstructed MP-FRAP system *in vitro*. Figure 1 shows a representative MP-FRAP recovery curve and associated fit generated with the new system. Our preliminary data compare favorably with accepted values found in the literature.

Figure 1:
A representative MP-FRAP recovery curve for 1 mg/ml FITC BSA in water and associated fit.

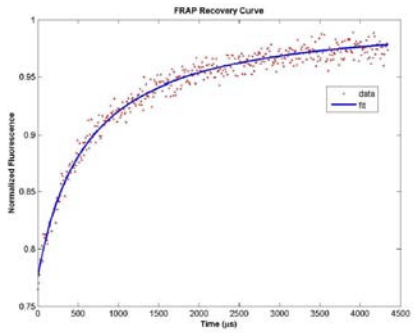

Figure 2:
Logarithmic plot of the bleach depth parameter, β, as a function of laser power. The line inserted on the graph indicates that $\beta \sim P^2$. The last data point can be seen to fall off from this line, and so represents the start of excitation saturation. Accurate MPFRAP is performed in the linear part of this curve.

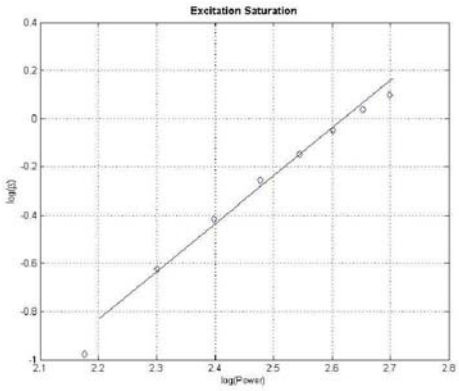

The MP-FRAP technique works by bleaching a region of interest and then monitoring the region as fluorescent molecules from outside the region diffuse in. In order to avoid bleaching during the monitor phase and excitation saturation during the bleaching phase, it is necessary to test several different monitor and bleach powers to set bounds on the laser powers that can be used for a give fluorescent probe and sample scattering depth. Excitation saturation describes the threshold beyond which increasing power to the sample yields diminishing returns in increased bleaching rates. Below this threshold, the bleach depth parameter, β, scales as the square of the bleaching power. Figure 2 is a logarithmic plot of the bleach depth parameter as a function of the laser power for FITC-BSA *in vitro*. The line inserted on the graph indicates that $\beta \sim P^2$. The last data point can be seen to fall off from this line, and so represents the minimum power at which excitation saturation occurs.

Our most significant undertaking of the past year has been a detailed theoretical study of the MP-FRAP recovery equation. This investigation began with the development of several MATLAB programs to generate and fit MP-FRAP data. Data is generated using the MP-FRAP with flow model, and then Poisson distributed random noise is added in an amount relative to the desired signal to noise ratio. We fit the data using a regressive fitting algorithm. With that procedure we have been asking the pivotal question: When does velocity become important to the fit? In other words, for what range of velocities does the convective flow significantly affect the characteristic diffusion time compared to that of a similar system without flow? We can test this by generating noisy data according to the flow model, then fitting these data using the model **without** flow. Figure 3 shows the results of this analysis. The abcissa describes the quality of fit as the ratio of the fitted τ_D to the input τ_D used to generate the data. The ordinate describes the span of normalized velocities over which the accuracy of the fit ranges from strong (τ_D fit / τ_D input ≈ 1) to poor (τ_D fit / τ_D input $\rightarrow 0$). Six values of τ_D

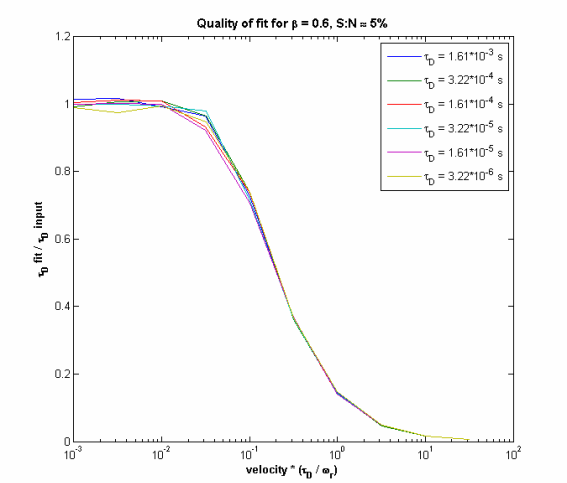

Figure 3:
Quality of fit for the characteristic diffusion time, τ_D, relative to a scaled velocity axis. The legend lists the values of the diffusion time used to generate the data. Error bars represent +/- 1 standard deviation.

for velocities ranging from 100 - 1000μm/s, were used to generate the data points in the figure. By inspection, we see that a good fit (τ_D fit / τ_D input $\geq$ 0.9) is achieved when the convective flow velocity is less than 0.05 (w_r/τ_D).

In year three, we will extend this analysis for other S/N ratios, then complete our theoretical analysis by determining what ranges of D,V,β, and S/N produce good fits for both D *and* V. This theoretical analysis will be accompanied by the experimental analysis described in the original tasks, now that the MPFRAP equipment is in its final, fully automated form. This task is behind schedule, but I anticipate its completion in Year 3.

Progress in Task 9.

The other early Task in the original Statement of Work is Task 9, which in its entirety is:

Task 9. Establish a reproducible measure of photodamage during a permeability measurement. (Years 1 and 2)

A. Evaluate systematic alterations in the fluorescence-versus-time curve as a reproducible measure of photodamage during permeability measurements.

B. Evaluate successive permeability measurements with distinct markers as a reproducible measure of photodamage during permeability measurements.

C. Evaluate second harmonic imaging of the adjacent matrix as a reproducible measure of photodamage during permeability measurements.

In pursuit of this task we evaluated second harmonic generation (SHG) signal from the extracellular matrix as a tool to measure photodamage during permeability measurements, as well as during MPFRAP measurements. The three fundamental optical properties we investigated were the backscattered SHG intensity, the ratio of forward scattered SHG to backscattered SHG, and "rho", a measure of the axial polarizing effects of collagen fibers. During this investigation of SHG signatures of breast tumor collagen, we realized that SHG can produce significant useful biological information about the matrix of the breast tumor in addition to being a measure of photodamage during MPSVP or MPFRAP. I will therefore discuss each of these three SHG properties in order, and focus on the interesting new directions we took our explorations, and why we did so:

Backscattered SHG Intensity Imaging of Fixed Pathology Specimens of Breast Tumors.

In discussions with Dr. Ping Tang of the Department of Pathology, we learned that there was currently no method available to predict which patients with identified Invasive Ductal Carcinoma would and would not metastasize. Based upon our experience with relaxin, and the fact that relaxin treatment simultaneously altered the SHG signature of tumors in mice[1] while increasing tumors' metastatic ability[2], we hypothesized that the metastatic ability of IDC tumors might be revealed in their SHG signatures. We quantified the average backscattered SHG intensity from 5 identified IDC regions in each of 7 thin fixed pathology sections (35 regions total) from patients whose IDCs had led to metastases, and an identical number from patients whose IDCs had not yet led to detectable metastases. Unfortunately, after some promising initial results, we found that there was no statistically significant difference between the backscattered SHG intensity of the two groups (661±212, N=35 IDC with Mets, 718±312, N=35 IDC without Mets), nor between the fractional area of SHG fibers above an arbitrary (but common) threshold (0.078±0.048, N=35 IDC with Mets, 0.089±0.082, N=35 IDC without Mets).

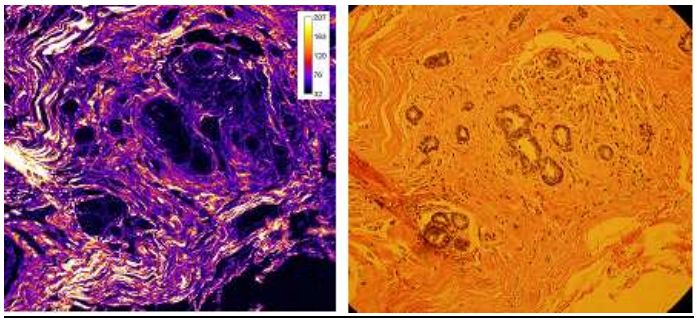

Fig 4 a) SHG image of fixed human breast tumor section
b) Digital camera picture of the same region in transmitted light, H and E stain.

We also determine that backscattered SHG did not distinguish between high grade and low grade DCIS (data not shown) nor between DCIS and IDC (data not shown).

Forward/Backwards Ratio of Fixed Pathology Specimens of Breast Tumors.

We also investigated the forward- versus backwards- scattering properties of breast tumor specimens. The ratio of forwards-scattered versus backwards-scattered signal (the F/B ratio) reveals the axial extent of the scattering structures. Historically when SHG is investigated in biological samples it is mainly applied to the rat tail tendon, an ideal sample of many well-aligned fibers of collagen I. In rat tails, Williams et al. showed that the F/B ratio was uniformly close to 1 even in fibers of widely varying diameters[3], an apparent contradiction solved by the determination that in that sample the fibers were only aligned (and hence SHG scatterers) in a thin shell around their surface, while their central cores were disordered (and hence not scattering). The F/B ratio remained 1 for different apparent fiber diameters because the thickness of the ordered shell was unchanged.

In our early explorations of SHG as a sensitive measure of photodamage, we hypothesized that F/B ratio may be a more sensitive indicator of matrix breakdown (due to its sensitivity to ordering) than backscattered SHG intensity. Figure 5 shows an F/B image of a thin section of a TG1-1 mouse mammary tumor grown in the mammary fat pad. Note the presence of a rich heterogeneous structure, with numerous fibers that are

significantly forward scattering (F/B can often exceed 10 in these samples). This is in marked contrast to the rat tail data with F/B ratio uniformly close to 1 in all fibers.

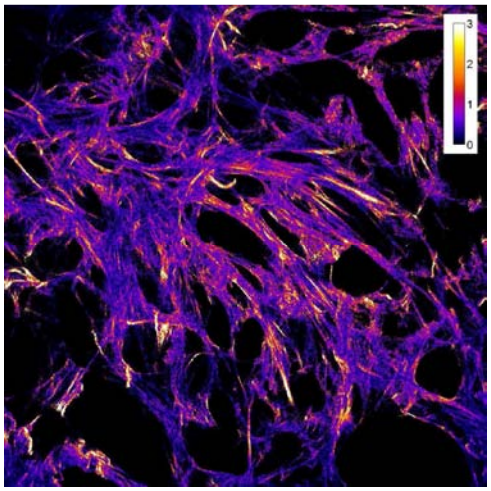

Fig 5. Forwards/Backwards SHG ratio of fresh TG1-1 tumor sections from a FVB mouse

These observations led us to realize that F/B ratio could be used to reveal new information about the processes of collagen synthesis and degradation with extremely high spatial resolution. Based upon our aforementioned discussions with Dr. Ping Tang, we are particularly interested in the insight SHG can produce into tumor metastatic ability. Our 2003 relaxin results suggest a relationship between collagen turnover and metastasis, while collagen turnover is likely to affect the ordering of individual collagen fibers: therefore we hypothesize that collagen metastatic ability will be related to the F/B ratio. We quantified the F/B ratio in five thin fixed sections of biopsies from patients with IDC, three with metastases and two without. There was no statistically significant difference in this preliminary data set: Mean F/B with met 18.3±11.1 (N=15) vs. mean F/B without met 20.5±12.3 (N=10), but we plan on testing our full sample set anyway, as well as explore unfixed tissue sections.

Polarization measurements of mouse collagen.

Our most significant efforts went into the measurement of the axial polarization effects of breast tumor collagen. In rat tail collagen Williams et al. and others have demonstrated that the angle between the polarization of the incoming laser and the collagen fiber, Θ, and the polarization of the outgoing SHG signal can be related by a simple equation:

$$I_y(\Theta) = I_p\left[\rho\cos^2\Theta + \sin^2\Theta\right]^2$$
$$I_x(\Theta) = I_p\left[\sin 2\Theta\right]^2$$

Where Iy and Ix are the polarization of the SHG signal parallel and perpendicular to the fiber, and rho is a fitting parameter. In certain symmetry conditions (i.e. a cylindrically symmetric distribution of single axis molecules, such as in fibrillar collagen[4]) rho is the ratio of the two independent elements of the hyperpolarizability matrix relating the incoming E field to the polarization of the fiber. Plotnikov et al. showed that rho is dictated by the angular orientation of the SHG scatterers (i.e. the collagen triple helix) relative to the fiber axis[4], so we hypothesized that this parameter could be an early indicator of subtle matrix damage during MPFRAP or SFAFRAP. Our first measurements were control measurements, where we measured rho in mouse tail collagen and compared to the literature. Interestingly, we measured a value of 1.27±0.31 (N=18) for mouse tail, versus the literature value[3] for rat tail collagen of 2.6±0.2. We subsequently confirmed that we do indeed get values comparable to literature values for

rat tail collagen (2.43±.31 N=12), which means that there is *something* intrinsically different between the axial polarizability of mouse tail versus rat tail collagen.

Our first hypothesis was that this difference in rho was due to a difference in the collagen 3 content, as literature suggests that collagen 3 content directly alters the angular orientation of triple helices in the overall fiber[5]. However, rho measurements in the mouse colon, which is known to contain a significant amount of collagen 3[5], produce the same rho (P=0.27) as in the mouse tail (1.14±0.4, N=25). Our current hypothesis is that intrinsic differences in the sequences of the collagen molecules, on a genetic level, produce these differences in rho. This suggests that even in pathological conditions such as breast cancer, the rho values in the tumor collagen will be indistinguishable from that in the host tissue. This has proven to be true: rho in collagen from TG1-1 mouse tumors grown in the mammary fat pad is indistinguishable from rho in the fat pad itself, and both are indistinguishable from the tail and colon data (TG1-1 rho: 1.23±0.39 N=20 and MFP rho: 1.44±0.25 N=5, P=0.24) (See Figure 6). Therefore, we believe that rho measurements are unlikely to offer any ability to *detect* tumor tissue (i.e. based upon differences in rho), but instead these results reveal that, in spite of the substantial difference in overall ECM density, MMP activity, etc., in tumor versus healthy tissue, the underlying collagen construction machinery is unchanged.

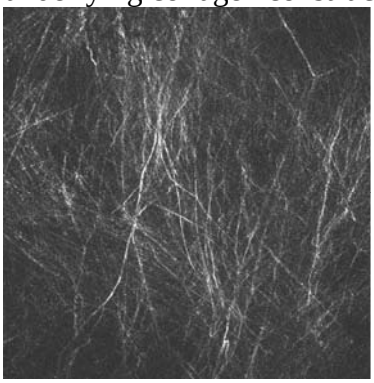

Figure 6a. SHG image of collagen in a TG1-1 tumor grown in the mammary fat pad.

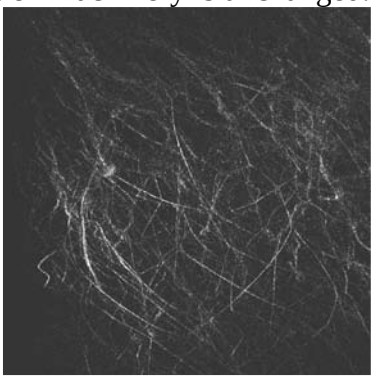

Figure 6b. SHG image of collagen in the mammary fat pad.

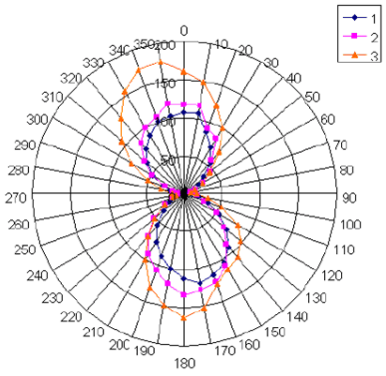

Figure 6c. Radar plot of signal vs. analyzer angle, used to determine rho.

Overall, this Task is behind schedule, because much of the effort that was originally devoted to determining how SHG can provide a measure of photodamage during MPFRAP has been diverted into extremely interesting exploration of the basic biology that optical properties of SHG signal reveal about the breast tumor ECM. We have learned that backscattered SHG intensity from fixed sections does not provide diagnostic information about the likelihood of a given IDC forming metastases, and that the axial polarizability of collagen seems to be a constant for all the collagen in a given animal. We have also learned that there is a rich heterogeneous structure apparent in the forwards/backwards ratio images of tumor collagen and that this forwards/backwards ratio may provide detailed information about the ordering properties of tumor collagen with high spatial resolution.

These observations formed the basis of a successful application for a prestigious Pew Young Investigator Award in the Biomedical Sciences. In that award we proposed to use forwards/backwards SHG imaging to understand the role of collagen structure in

breast tumor metastasis, and determine if one of several forwards/backwards imaging devices we will produce will allow us to predict metastatic ability in breast tumors. As a result of winning this award, exploration of these complex SHG properties in breast tumors will be "spun off" into a new project under that grant, and we can return to the original goal of this Task, to measure photodamage during an MPFRAP or SVP experiment.

Progress in Task 8.

Chronologically, the next Task in the Statement of Work is Task 8, which in its entirety is:

Task 8. Establish the allowed volume for accurate permeability measurements in the parameter space of i) average vessel permeability, ii) average tissue diffusion coefficient of fluorescent tracer, and iii) mean distance between vessels. (Years 2 and 3)

A. Perform extensive mathematical modeling to determine the allowed volume in parameter space.

B. Perform measurements of permeability, diffusion coefficients, and intravessel distances in tumor vessels to test the predictions of the model.

C. Determine where in parameter space, on average, several key experimental tumor types lie.

We have devoted the first year on this Task to aim A. We have determined the correct mathematical model of the concentration profile of a tumor vessel extravasating a fluorescent tracer. The geometry of this model, a region bounded internally by a cylindrical surface, reflects the geometry of the space in a tumor immediately surrounding a tumor vessel. The equation for this concentration profile as a function of time and radial distance is as follows:

$$C(r,t) = C_i[(\frac{a}{r})^{1/2} erfc(\frac{r-a}{2\sqrt{Dt}}) + \frac{(r-a)(Dt)^{1/2}}{4r^{3/2}a^{1/2}} ierfc(\frac{r-a}{2\sqrt{Dt}}) + \frac{Dt(9a^2-2ar-7r^2)}{32a^{3/2}r^{5/2}} i^2 erfc(\frac{r-a}{2\sqrt{Dt}})]$$

This equation is a truncated infinite series, in which only the first three terms were found to make a significant contribution to the overall result. The parameter C_i, the interstitial concentration of fluorescent tracer at the external surface of the vessel wall, is calculated by the following equation:

$$C_i = \frac{(1-\sigma)C_p}{1-\sigma e^{-Pe}}$$

The parameter C_p in this equation is the plasma (intravenous) concentration of fluorescent tracer, which is estimated at 1.47 nM based on the average volume of blood present in an adult mouse and the amount of fluorescent tracer typically injected into the mouse during a permeability experiment. Pe, a dimensionless number relating advection to diffusion, has been discovered by Sarelius et al to be on the order of .1 for venules and .2 for arterioles[6]. An intermediate value of .15 was chosen for the purposes of this model. σ, the reflection coefficient, is a quantity that takes into account the physical hindrance that the vessel wall affords to macromolecular diffusion. In vessels of the skin (the most appropriate location given our *in vivo* imaging techniques), Reed et al determined σ to be approximately .94, which was the value used in this model as well[7]. Given these parameters, C_i is calculated as 0.46 nM.

The computer program MATLAB was used to calculate concentration profiles for tumor vessels with various average tissue diffusion coefficients reflecting those found in several commonly studied tumor lines when perfused with FITC-BSA in a permeability experiment[8]. The profiles were calculated by MATLAB, then integrated to yield the total number of moles of fluorescent tracer released over the chosen time period. As tumor vessels are on average approximately 10 microns in diameter and set in 50 um opposition to one another, profiles were calculated for two vessels fitting these criteria to determine the extent to which extravasated material from the two vessels overlaps. This overlap would result in a higher measurement of fluorescent intensity, which in turn results in erroneously high measurements of vascular permeability. Figure 7 represents a typical calculated concentration profile of vessels from a U87 glioma, which has a FITC-BSA diffusion coefficient of 2.2×10^{-7} cm^2/s. This relatively low interstitial diffusion coefficient produces a ~3% overlap in extravasation at the 15 second time point chosen (a typical observation time for MPSVP measurements). As the interstitial diffusion coefficient increases, the percentage overlap (and hence expected error in MPSVP measurements) increases: HSTS26T human soft tissue sarcoma, with a FITC-BSA diffusion coefficient of 3.5x10-7 cm^2/s has ~7% overlap, while LS174T human colorectal carcinoma or MCaIV murine mammary adenocarcinoma, with a FITC-BSA diffusion coefficient of 4.5×10^{-7} cm^2/s has a ~10% overlap.

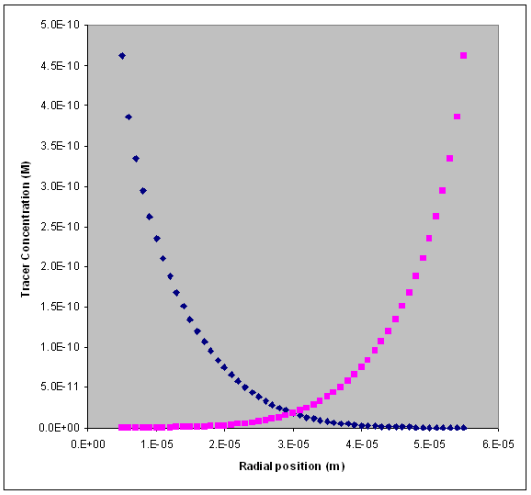

Figure 7: 10-um diameter vessels at 50 um separation in a hypothetical U87 glioma, with a FITC-BSA diffusion coefficient of 2.2×10^{-7} cm^2/s.

This series of calculations show that in all considered cases of average tissue diffusion coefficient, some error in the measurement of permeability is to be expected when measuring the fluorescent intensity in the interstitium between two tumor vessels. This amounts to approximately a 10% overage in the low-collagen, high-diffusion LS174T and MCaIV tumors. As relative collagen content of tumors can be measured *in vivo* using our techniques for quantitation of second harmonic generation signal or chemical methods, it is possible to predict approximately how much overlap will be present in any given tumor line. Figure 8 illustrates this concept.

If we allow for a maximum overlap error of 10% as a metric for determining whether or not a permeability measurement is accurate, we find that distance between vessels has a marked effect on the extent to which the permeability measurement can be compromised. This effect was studied by varying the distance between vessels assuming a U87 glioma ($D = 2.2 \times 10^{-7}$ cm^2/s) as the tumor of interest – a type chosen for its low levels of predicted overlap at physiological norms as shown in Figure 7. Figure 9 shows the increases in percent overlap as intravascular distance decreases in U87 glioma.

This series of calculations shows that variation in overlap error is much more dramatic when vessel distance is the altered parameter (as opposed to the previous series in which diffusion coefficient is altered). As tumor vascular beds are by nature chaotic

and unpatterned, all of these intravascular distances are reasonably likely to be present in a given tumor. This relation indicates that if we wish to maintain a maximum of 10% error in the permeability measurement for a low-diffusion tumor type such as U87 glioma, vessels measured for permeability cannot be closer than approximately 35 um from their nearest neighbor. This number will by necessity increase when faced with higher-diffusion tumor types such as MCaIV and LS174T.

Overall, we have made significant progress in Task 8, which in the original statement of work was expected to commence in the beginning of year 2 and finish at the end of year 3. With the most onerous portion of that Task, Aim 8A, almost complete, in my estimation this Task is slightly ahead of schedule.

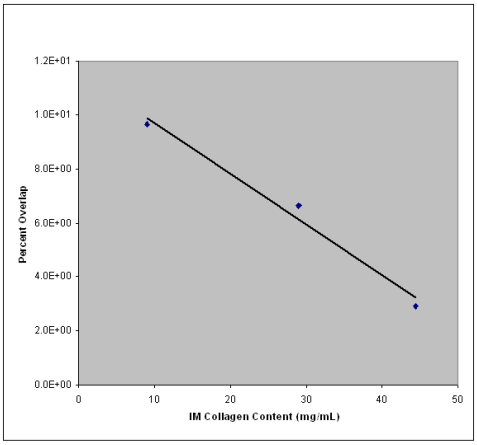

Figure 8: Plot of calculated overlap error in permeability measurement versus interstitial matrix (IM) collagen content. Several of our standard tumor models lie in this range (LS174T, MCaIV, HSTS, and U87). Calculated for 10 um vessels spaced 50 um apart, at 15 seconds after injection.

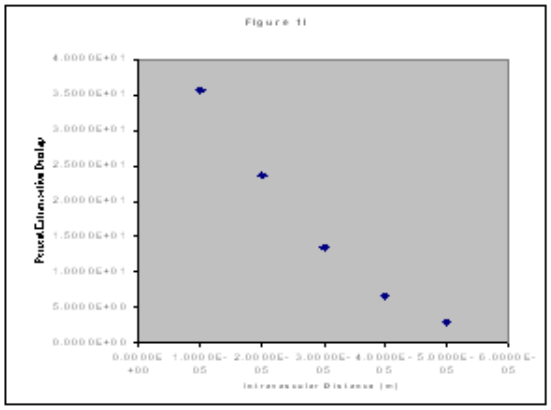

Figure 9: Plot of expected percent error in permeability measurement as a function of intravascular distance in U87 glioma.

Progress in Tasks 1-6.

The other Tasks in the original Statement of Work are intended to start in year 3 or later, but we have already made substantive progress on several of them. All six of these upcoming tasks have three key common steps: the growth of tumors in dorsal skinfold chambers, the loading of ECs in those tumors with a fluorescent calcium indicator, and the stable perfusion of pharmacological agents onto those samples without motion artifacts. These three steps, and their consistent and reproducible performance, has absorbed the lion's share of our time over the past year, as many of the "temporary" practices and techniques used to originally perform these tasks have proven unsuitable for consistent "mass production" of data by multiple laboratory members.

Dorsal skinfold chambers: Generating decent dorsal skinfold chambers in sufficient numbers has proven to be one of the key stumbling blocks. Originally only the PI, Edward Brown, had the necessary years of practice to produce good chambers, and while those were sufficient for our first year of growing the lab, it has been necessary to devote significant amounts of time every week for the other lab personnel to practice this

difficult surgery. Two lab members are now consistently able to produce good chambers, while the other two still need more practice. We are also hiring a laboratory technician who will devote two days or more per week solely to making chambers, although they will probably not be of sufficient quality to use for another six months to a year.

Loading ECs *in vivo* with fluorescent indicator dye: Generating consistent, *reproducible* loading of TECs with a calcium indicator dye has also proven to be a hurdle. After extensive practice and modification of the recipes we are now able to get more consistent (but still far from perfect: we will likely always be tweaking this recipe) loading of TECs *in vivo* (Figure 10). Interestingly, we have found that fura preferentially loads ECs in the healthy skin of the dorsal skinfold chamber: if this holds true in tumors, many of our previous plans to utilize TIE2-GFP mice as well as complex FRET based genetic indicators will be moot.

Stable perfusion of reagents: Our previous method of manual pippetting of reagents onto the sample dish or dorsal skinfold chamber produced a level of sample motion that was incompatible with the high optical sectioning of the MPLSM. As will be discussed in Task 2 below, this was solved with purchase of, and extensive practice with, a new multichannel perfusion system. This has allowed us to generate requisite preliminary data for Tasks 1-6, such as dose-response curves for ECs *in vitro*, as shown in Figure 11.

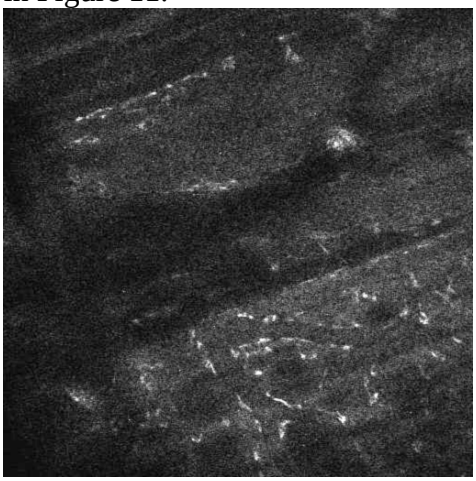

Figure 10. MPLSM image of *in vivo* ECs labeled with fura application. The exposed skin of a dorsal skinfold chamber was treated with fura loading solution then washed. A branched network of vessels with labeled ECs is visible in the lower right. Image is 600 microns across.

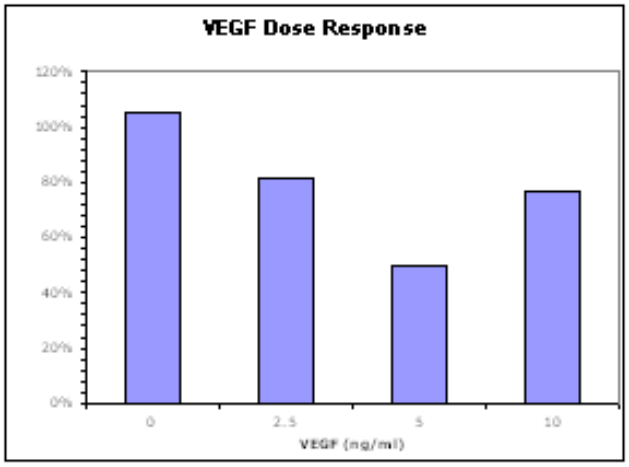

Figure 11. Dose-response curve of fura-loaded BAECs to VEGF *in vitro*. Our new perfusion system allows stable application of reagents and hence the production of data such as this. The mean FL intensity of cells at 80% confluence was used, and the last 20 scans of the time series (after VEGF) was divided by the mean FL intensity of the first 20 scans (before VEGF).

I will now discuss specific progress related to two particular tasks.
Task 1, in its entirety, is:

Task 1. Determine role of external calcium influx on translation of VEGFR2 activation to tumor endothelial cell (TEC) calcium signals and tumor vessel permeability. (Year 3)

A. Apply NiCl (blocks plasmalemmal calcium channels) and $CaCl_2$ to a tumor vessel via pipette and observe the TEC calcium response and subsequent permeability change.
B. Elevate TEC calcium and vascular permeability with extrinsic VEGF then attempt to block this elevation by repeating with NiCl.
C. Reduce TEC calcium and vascular permeability with VEGF blockade and attempt to recover baseline calcium and permeability with $CaCl_2$.

As stated in last year's progress report, *in vitro* pilot studies corresponding to each of the *in vivo* tasks relating to the development of pharmacological reagents to impede angiogenic signaling must be undertaken as appropriate controls and standards for comparison. Task 1A, the application of $NiCl_2$ to endothelial cells to determine the effect of external calcium influx on angiogenic signaling, is the subject of one of these pilot studies. Divalent nickel as a cation is physiologically harmful to cells at elevated levels in both acute and chronic exposures, but it is suggested by at least one group engaged in cationic blockade studies that levels as high as 2 mM are required for successful block of plasmalemmal calcium channels[9]. To determine the effect of these high NiCl2 levels on the health of the endothelial cells studied, viability assays were performed on bovine aortic endothelial cells (BAECs) and immortalized mouse pancreatic endothelial cells that produce hemangiomas (MS1/SVEN1 line). The goal of this study was to determine the acute toxicity level of divalent nickel on normal and tumor endothelial cells, as well as to determine whether or not TECs would exhibit behavior different from normal ECs when exposed to divalent nickel. Figures 12A and 12B are tables of percent viability as assayed by trypan blue exclusion.

Figure 12a Percent viability as a function of nickel concentration in BAECs. Each concentration was assayed in quadruplicate, for a total n=24 in 6 groups of n=4. Nickel chloride was added in solution in growth medium and cells were exposed to the medium for 30 minutes, then washed once. The trypan blue stain was performed on trypsinized cells seeded in a 24-well plate at $1x10^5$ cells per well.

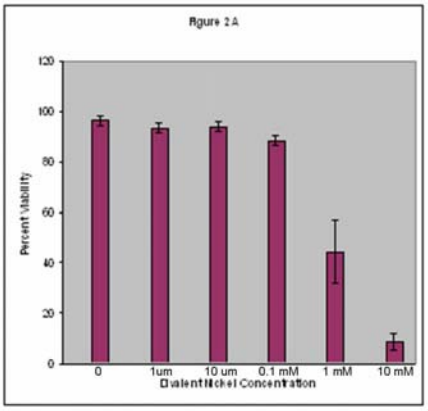

Figure 12b Percent viability as a function of nickel concentration in MS1/SVEN1 ECs.

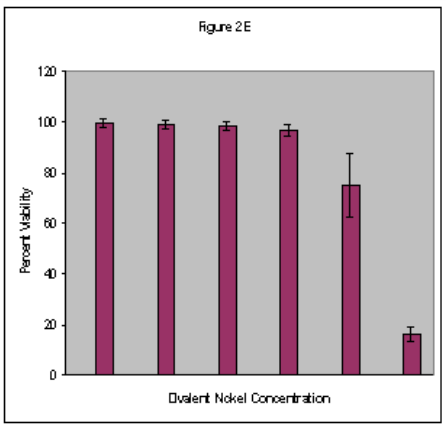

It is clear from these two figures that viability of endothelial cells is decreased by a statistically significant amount by the use of 1 mM $NiCl_2$ solution in medium regardless of the origin of the endothelial cells (primary or immortalized). The end result of this assay was to determine that a concentration of 0.1 mM, or one-tenth that suggested for successful cationic block, was more appropriate to use in a physiological setting. Likewise, these results seem to suggest that normal and tumor-derived endothelial cells have similar tolerances for acute divalent nickel exposure.

Subsequent to the establishment of safe levels of divalent nickel for use in the *in vitro* pilot study for Task 1, an experiment was performed to determine the extent to which safe levels of divalent nickel was actually able to block extracellular calcium influx in immortalized MS1/SVEN1 murine pancreatic endothelial cells. MS1/SVEN1 cells at $1x10^5$ cells per well in a 96-well plate were loaded with the calcium indicator dye Fluo-4 and subjected to three treatment regimens (n=15 each): control (saline only), 30 uM Na-ATP to induce extracellular calcium influx, and 30 um Na-ATP with .1 mM $NiCl_2$. Reagents were manually pipetted at 100 uL/well and the plate was excited at 480 nm (bandpass of 20 nm). Fluorescent intensities were collected at 530 nm (bandpass of 20 nm). Figure 13 shows the results, revealing that these low but safe levels of NiCl2 are sufficient to block influx of external calcium.

Figure 13. Demonstration that safe levels of NiCl2 can block ATP induced influx of external calcium in BAECs. ATP alone is statistically significantly different from both Control and ATP+NiCl (P<0.0001).

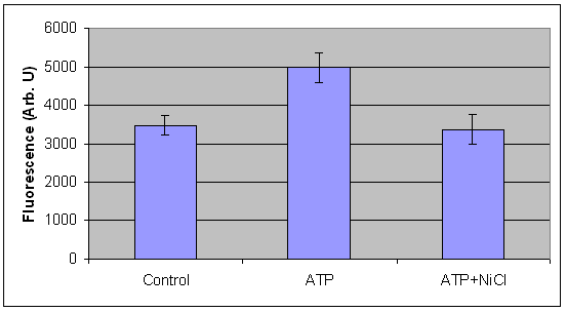

Task 2, in its entirety, is:

Task 2. To determine the role of diacylglycerol (DAG) in translation of VEGFR2 activation to TEC calcium signals and tumor vessel permeability. (Year 3)

A. Apply OAG (a DAG analog) and U73122 (a PLCγ inhibitor) and observe the calcium response in TECs as well as monitor subsequent vascular permeability changes.

B. Elevate TEC calcium and vascular permeability with extrinsic VEGF via pipette administration, and attempt to block this elevation by repeating with DAG inhibitor.

C. Reduce TEC calcium levels and vascular permeability with VEGF blockade, and attempt to recover baseline TEC calcium and vascular permeability with OAG.

In pursuit of this task we have been investigating the application of OAG, VEGF, and U73122 to BAECs *in vitro* and monitoring the subsequent calcium response. One of the most time-consuming parts of this has been the construction and practice using a complex multichannel perfusion system, as we found that manual pipetting of reagents produced sample motion that was incompatible with the extremely fine optical sectioning

of the MPLSM. Figure 14 shows a typical calcium response after application of OAG, with subsequent recovery after OAG removal, using the new perfusion system.

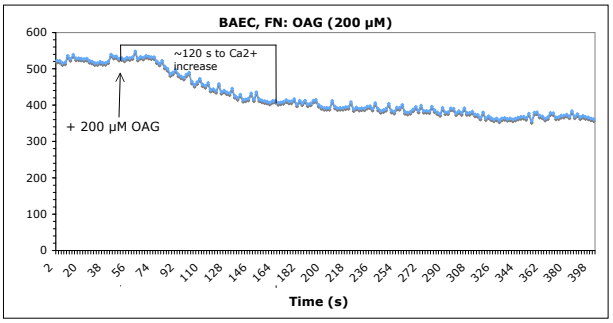

Figure 14a. OAG, a diacylglycerol analog, increases calcium in fura-loaded bovine aortic endothelial cells. This increase in calcium is represented by a decrease in fura fluorescence.

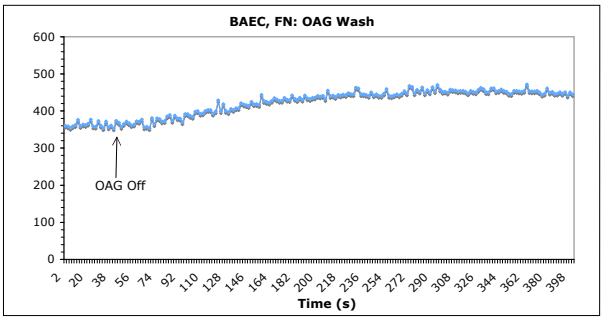

Figure 14b. After washout of OAG, fura fluorescence recovers to previous values.

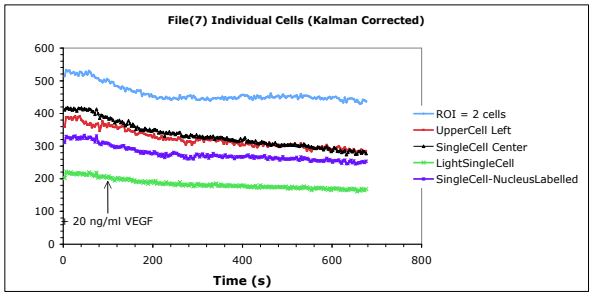

Figure 14c. VEGF increases calcium in fura-loaded bovine aortic endothelial cells. The blue line is two contiguous cells, the remaining lines are individual cells. This increase in calcium is represented by a decrease in fura fluorescence.

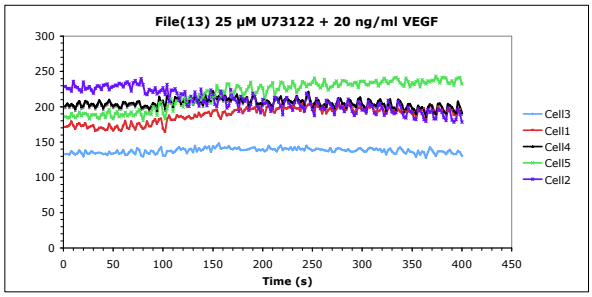

Figure 14d. Pre-incubation of BAECs with 25 µM U73122 prevents the response to VEGF.

These results demonstrate 1) that these levels of OAG, VEGF, and U73122 can induce and block a calcium response in BAECs and hence suggest that they are suitable levels for use with tumor endothelial cells 2) that BAECS have the machinery to respond to intrinsic DAG signals, and that VEGF utilizes PLCgamma to induce its calcium response in this cell type 3) that our MPLSM can record long-time-trace calcium signals with fura fluorescence without significant photobleaching, and 4) we can do so without sample motion artifacts when reagents are perfused.

Key Research Accomplishments in the previous year:

1) Made significant progress in Task 7, by construction and testing of the final form of the MPFRAP rig, measurement of key experimental parameters, and theoretical analysis of the effects of different flows on the fitting error using a diffusion-only formula.

2) Made significant progress in Task 8, by determination of the formula describing the concentration of fluorescent dye outside of a vessel, and use of that formula to evaluate the concentration of indicator apparently from the vessel studied with MPSVP that is actually from adjacent vessels (hence producing errors in the measured permeability) and an analysis of this error due to variations in diffusive hindrance and vessel proximity.

3) Utilized work on Task 9c (the evaluation of second harmonic imaging of the local matrix as a reproducible measure of photodamage during MPFRAP and permeability measurements) to commence a new, funded, research program investigating the complex optical signatures of SHG in breast tumor tissue, its relationship to breast tumor metastasis, and its ability to predict metastatic ability.

4) Performed extensive training and practice in dorsal skinfold chamber production, evaluation of TEC dye loading, and development of protocols for a new perfusion system, which will allow reproducible results in Tasks 1-6, which are only scheduled to commence now.

5) Produced important preliminary data for upcoming Tasks 1 and 2.

Reportable Outcomes:

Over the past year I have given two invited talks, one of which was part of the BCRP LINKS meeting for this grant:

"Angiogenic Signaling in Living Breast Tumor Models" Invited lecture presented at the BCRP LINKS meeting, Baltimore, MD, 2006

"Multiphoton Laser-Scanning Microscopy of Tumor biology" Invited lecture presented at the Department of Physics, Ithaca College, Ithaca, NY, 2007

I have also won two grants while supported by this award. The first, "The influence of neuronal activity on breast tumor metastasis to the brain" is a Department of Defence BCRP Synergistic Idea Award in which I am co-PI with 20% effort. This two year $250k direct cost award has as its goal to utilize insights gained from the study of dendritic spine motility to discover novel reagents that inhibit breast tumor metastases in the brain. This represents a collaboration between myself and Dr. Ania Majewska of the Department of Neurobiology and Behavior.

The second grant is "Dynamic *in vivo* imaging and quantification of collagen microstructure and turnover in breast tumor models." This is a prestigious Pew Scholar in the Biomedical Sciences Award in which I am PI with 9% effort. This four year $250k direct costs award has as its goal to investigate collagen turnover in breast tumor models using novel microscopy techniques. This is specifically a "spin-off" of our work on Task

9, where we used SHG imaging to study the breast tumor extracellular matrix during permeability and MPFRAP measurements. We will now use SHG to understand the relationship between the tumor ECM and metastasis.

I feel that the content of these grant applications are noteworthy in that they show that the Era of hope Scholar Award has produced a long-term commitment to breast cancer research in my laboratory and has allowed me to attract other scientists (i..e. Dr. Majewska of the Department of Neurobiology and Anatomy, P.I. of the aforementioned Synergistic Idea Award application) to breast cancer research.

Conclusion

Overall we are behind schedule in two Tasks (one of which has "spun off" an entirely new funded avenue of breast cancer research for the lab), slightly ahead of schedule in one Task, and significantly ahead of schedule in six Tasks. In conclusion, I believe that I have made significant progress on the goals outlined in my Era of Hope Scholar Award.

References

1. Brown, E. et al. Dynamic imaging of collagen and its modulation in tumors in vivo using second harmonic generation. Nat Med 9, 796-801 (2003).
2. Silvertown, J. D., Geddes, B. J. & Summerlee, A. J. Adenovirus-mediated expression of human prorelaxin promotes the invasive potential of canine mammary cancer cells. Endocrinology 144, 3683-91 (2003).
3. Williams, R. M., Zipfel, W. R. & Webb, W. W. Interpreting second-harmonic generation images of collagen I fibrils. Biophys J 88, 1377-86 (2005).
4. Plotnikov, S. V., Millard, A. C., Campagnola, P. J. & Mohler, W. A. Characterization of the myosin-based source for second-harmonic generation from muscle sarcomeres. Biophys J 90, 693-703 (2006).
5. Cameron, G. J., Alberts, I. L., Laing, J. H. & Wess, T. J. Structure of type I and type III heterotypic collagen fibrils: an X-ray diffraction study. J Struct Biol 137, 15-22 (2002).
6. Sarelius, I. H., Kuebel, J. M., Wang, J. & Huxley, V. H. Macromolecule permeability of in situ and excised rodent skeletal muscle arterioles and venules. Am J Physiol Heart Circ Physiol 290, H474-80 (2006).
7. Reed, R. K., Townsley, M. I. & Taylor, A. E. Estimation of capillary reflection coefficients and unique PS products in dog paw. Am J Physiol 257, H1037-41 (1989).
8. Ramanujan, S. et al. Diffusion and convection in collagen gels: implications for transport in the tumor interstitium. Biophys J 83, 1650-60 (2002).
9. Zweifach, A. & Lewis, R. S. Calcium-dependent potentiation of store-operated calcium channels in T lymphocytes. J Gen Physiol 107, 597-610 (1996).

Curriculum Vitae

General Information:

Name: Edward Brown III, PhD

Office Address: Department of Biomedical Engineering
601 Elmwood Ave, Box 639
University of Rochester Medical Center
Rochester, NY, 14642

E-mail: edward_brown@urmc.rochester.edu

Phone: 585 273-5918 **Fax:** 585 273-4746

Educational Background:

BS Magna Cum Laude with Honors in	Physics	Wake Forest University	1992
MS	Physics	Cornell University	1995
PhD	Physics	Cornell University	1999

Professional Positions:

Doctoral Training

Graduate Student, Department of Physics, Cornell University
Laboratory of Dr. Watt Webb June 1992-July 1999

Post-Doctoral Fellow, Department of Radiation Oncology, Harvard Medical School
Massachusetts General Hospital
Laboratory of Dr. Rakesh Jain July 1999 – December 2001
Recipient of NRSA F32 Postdoctoral Research Award July 2000 - June 2002

Academic Positions

Instructor, Department of Radiation Oncology, Harvard Medical School
Massachusetts General Hospital January 2002-June 2005
Recipient of Whitaker Biomedical Engineering Research Grant July 2003
Recipient of American Cancer Society Institutional Research Grant July 2003
Assistant Professor, Department of Biomedical Engineering, University of Rochester Medical Center September 2005-
Recipient of Department of Defense Era of Hope Scholar Award September 2005
Recipient of Pew Scholars in the Biomedical Sciences Award June 2007

Professional Memberships:

Biophysical Society	1995 -
American Association for Cancer Research	1999 –
Optical Society of America	2006-

Awards and Honors:

National Merit Scholarship	1988
Reynolds Scholarship - Wake Forest University (full tuition/room/board, stipend)	1988 - 1992
Phi Beta Kappa	1992
Omicron Delta Kappa, National Service Honor Society	1992
President, Sigma Pi Sigma WFU chapter National Physics Honor Society	1992
President, Alpha Phi Omega WFU chapter National Service Fraternity	1992
Speas Award for Excellence in Physics	1992
AFLAC-AACR Scholars in Cancer Research Award	2000
Department of Defense Era of Hope Scholar Award	2005 –
Pew Scholar in the Biomedical Sciences Award	2007-

National Service Responsibilities:

Scientist Reviewer - Grant Review Panel, Department of Defense
Breast Cancer Research Program, Vienna, VA, 2002, 2004, 2007
Scientist Reviewer - Hypertension and Microcirculation NIH Study Section, 2004
Scientist Reviewer - URMC Johnson and Johnson Discovery Concept Fund, 2005, 2006
Advisory Board - Nebraska Center for Cell Biology, 2004 -
Served as reviewer for Applied Optics, Biophysical Journal, Cancer Research, Journal of Biomedical Optics, Microcirculation, Microvascular Research, Nature Methods, Optics Express, Optics Letters, Photochemistry and Photobiology, Biomechanics, Journal of Microscopy.

Teaching Experience:

Teaching Assistant, Cornell University Department of Physics 1992, 1993
Physics 213 Electricity and Magnetism
Physics 214 Waves and Optics

Instructor, Cold Spring Harbor Laboratory summer course 1995 - 1998
Four courses entitled “Imaging Structure and Function in the Nervous System”
Lectured on and demonstrated the use of the Multiphoton Laser Scanning Microscope

Course Organizer - “Methods in Biomedical Engineering” 2001 - 2003
Organized Steele Laboratory course, designed syllabus, lectured on light microscopy, fluorescence photobleaching recovery, and multiphoton microscopy

Lecturer, MIT Chemical Engineering, Course 10.548J 2003
Course entitled "Tumor Pathophysiology and Transport Phenomena"
Lectured on *in vivo* multiphoton microscopy

Lecturer, University of Rochester Institute of Optics, Optics 476 2005
Course entitled “Biomedical Optics”
Lectured on *in vivo* multiphoton microscopy

Lecturer, University of Rochester Institute of Optics Summer Courses 2005-
Courses entitled “ Biomedical Optics” and “High-Resolution Microscopy”
Lectured on epifluorescence, confocal, and multiphoton microscopy

Student Supervision
Supervised a total of 5 undergraduates who were either (2) paid for summer work or received credit through the MIT UROP program (2) or UR Independent Study Credits

Graduate Student Supervision
Provided direct supervision for three graduate students (two M.I.T. Ph.D. candidates and one Harvard Medical School M.D.-Ph.D. candidate) 1999-2005

Currently supervising one University of Rochester Ph.D. candidate from the Department of Physics, one from the Institute of Optics, and one from the Biomedical Engineering Department 2005-

Other Supervision
Currently supervising one Research Assistant Professor from the Biomedical Engineering Department 2005-

Publications:
Peer-Reviewed Journals:

Shear J, **Brown E**, Webb W. (1996) Multiphoton-excited fluorescence of fluorogen-labeled neurotransmitters. *Anal Chem* 68(10) 1778-1783.

Brown E, Shear J, Adams S, Tsien R, Webb W. (1999) Photolysis of caged calcium in femtoliter volumes using two-photon excitation. *Biophysical Journal* 76, 489-499.

Brown E, Wu E-S, Zipfel W, Webb W. (1999) Measurement of molecular diffusion in solution by multiphoton fluorescence photobleaching recovery. *Biophysical Journal* 77, 2837-2849.

Majewska A, **Brown E**, Ross J, Yuste R. (2000) Mechanisms of calcium decay kinetics in hippocampal spines: role of spine calcium pumps and calcium diffusion through the spine neck in biochemical compartmentalization. *J Neuroscience* 20(5):1722-1734.

Pluen A, Boucher Y, Ramanujan S, McKee TD, Gohongi T, di Tomaso E, **Brown E**, Izumi Y, Campbell R, Berk D, Jain RK. (2001) Role of tumor-host interactions in interstitial

diffusion of macromolecules: cranial vs. subcutaneous tumors. *Proc Natl Acad Sci.* Apr 10;98(8):4628-33.

Brown E, Campbell R, Tsuzuki Y, Xu L, Carmeliet P, Fukumura D, Jain RK. (2001) *In vivo* measurement of gene expression, angiogenesis, and physiological function in tumors using multiphoton laser scanning microscopy. *Nature Medicine* 7(7): 864-868.

Migliorini C, Qian Y, Chen H, **Brown E**, Jain RK, Munn L. (2002) Red blood cells augment leukocyte rolling in a virtual blood vessel. *Biophysical Journal* 83, 1834-41.

Ramanujan S, Pluen A, McKee T, **Brown E**, Boucher Y. Jain RK. (2002) Diffusion and convection in collagen gels: relation to transport hindrance in the tumor. *Biophysical Journal* 83, 1650-1660.

Padera T, Kadambi A, di Tomaso E, Mouta-Carreira C, **Brown E**, Boucher Y, Choi N, Mathisen D, Wain J, Mark E, Munn L, Jain RK. (2002) Lymphatic metastasis in the absence of functional intratumor lymphatics. *Science* Jun 7;296(5574):1883-6.

Campbell R, Fukumura D, **Brown E**, Mazzola L, Izumi Y, Jain RK, Torchilin V, Munn L. (2002) Cationic charge determines the distribution of liposomes between the vascular and extravascular compartments of tumors. *Cancer Research* 62(23):6831-6.

Wei X, Henke V, Strübing C, **Brown E**, Clapham D. (2003) Real time imaging of nuclear permeation by EGFP in single intact cells. *Biophysical Journal* 84:1317-1327.

Schmidt H, **Brown E**, Schwaller B, Eilers J. (2003) Diffusional mobility of parvalbumin in spiny dendrites of cerebellar Purkinje neurons quantified by fluorescence recovery after photobleaching *Biophysical Journal* 84:2599-2608.

Brown E*, McKee T*, di Tomaso E, Pluen A, Seed B, Boucher Y, Jain RK. (2003) Dynamic imaging of collagen and its modulation in tumors *in vivo* using second harmonic generation. *Nature Medicine* 9(6):796-801 *contributed equally.

Abdul-Karim A, Al-Kofahi K, **Brown E**, Jain RK, Roysam B. (2003) Automated tracing and change analysis of angiogenic vasculature from *in vivo* multiphoton image time series. *Microvascular Research* 66(2):113-125

Znati C, Rosenstein M, McKee T, **Brown E**, Turner D, Bloomer WD, Watkins S, Jain RK, Boucher Y. (2003) Irradiation Reduces Interstitial Fluid Transport and Increases the Collagen Content in Tumors. *Clin Cancer Res* 9:5508-5513

Alexandrakis G, **Brown E**, Tong R, McKee T, Campbell R, Boucher Y, Jain RK. (2004) Two-photon fluorescence correlation microscopy to quantify the transport of fluorescently labeled tracers in tumors. *Nature Medicine* 10(2):203-207.

Garkavtsev I, Kozin S, Chernova O, Xu L, **Brown E**, Barnett G, Jain RK. (2004) *ING4:* a novel regulator of brain tumor growth and angiogenesis. *Nature* 428:328-332.

Brown E, Boucher Y, Nasser S, Jain RK. (2004) Measurement of macromolecular diffusion coefficients in human tumors. *Microvascular Research* 67(3):231-236

Duda D, Fukumura D, Munn L, Booth M, **Brown E**, Huang P, Seed B, Jain RK (2004) Differential transplantability of tumor-associated stromal cells *Cancer Research* 64: 5920-5924

Stroh M, Zimmer J, Duda D, Levchenko T, Cohen K, **Brown E**, Scadden D, Torchilin V, Bawendi M, Fukumura D, and Jain RK. (2005) Quantum dots spectrally distinguish multiple species within the tumor milieu in vivo. *Nature Medicin*e 11(6):678-682

Tyrrell J, Mahadevan V, Tong R, **Brown E**, Jain RK, Roysam B. (2005) 3D model-based complexity analysis of tumor microvasculature from *in vivo* multiphoton Images. *Microvascular Research* 70(3):165-178

Schmidt H, Arendt O, **Brown E**, Schwaller B, Eilers J. (2007) Parvalbumin is freely mobile in axons, somata, and nuclei of cerebellar Purkinje neurons. *J. Neurochem.* 100:727-735

Book chapters:

Brown E, Webb W. (1998) Two-Photon Activation of Caged Calcium with Submicron, Submillisecond Resolution. In Mariott G (ed). Caged Compounds. Methods of Enzymology series v. 291 Academic Press, San Diego. pp. 356-380

Jain RK, **Brown E**, Munn L, Fukumura D. (2004) Intravital Microscopy of Normal and Diseased Tissue in the Mouse. In: Spector D, Goldman R. (eds). Live Cell Imaging: A Laboratory Manual. Cold Spring Harbor Laboratory Press, Cold Spring Harbor, New York. Chapter 24, pp 435-466.

Brown E, Majewska A, Jain RK. (2005) FRAP and Multiphoton FRAP. In: Yuste R, Konnerth A. (eds). Imaging in Neuroscience and Development: A Laboratory Manual. Cold Spring Harbor Laboratory Press, Cold Spring Harbor, New York. Chapter 56, pp. 429-438.

Brown E, Munn L, Fukumura D, Jain RK.(2005) A Practical Guide to *in vivo* Imaging of Tumors. In: Yuste R, Konnerth A. (eds). Imaging in Neuroscience and Development: A Laboratory Manual. Cold Spring Harbor Laboratory Press, Cold Spring Harbor, New York. Chapter 92, pp. 695-700.

Jain RK, Fukumura D, Munn L, **Brown E** (2007) Optical Microscopy in Small Animal Research. In: Tavitian B., Leroy-Willig A., Ntziachristos V. (ed) Imaging of Vertebrates. Wiley & Sons London, UK *In Press*

Jain RK, Fukumura D, Munn L, **Brown E** (2007) Tumor Angiogenesis and Blood Flow. In: Tavitian B., Leroy-Willig A., Ntziachristos V. (ed) Imaging of Vertebrates. Wiley & Sons London, UK *In Press*

Brown E, Majewska A, Jain RK (2007) Photobleaching and Recovery with Nonlinear Microscopy. In: So P., Masters B. (eds) Handbook of Biological Nonlinear Optical Microscopy. Oxford University Press, Oxford UK. *In Press*

Jain RK, Booth M, Padera T, Munn L, Fukumura D, **Brown E**. (2007) Applications of Nonlinear Intravital Microscopy in Tumor Biology. In: So P., Masters B. (eds) Handbook of Biological Nonlinear Optical Microscopy. Oxford University Press, Oxford UK. *In Press*

Funding History
Ongoing Research Support:

"Angiogenic Signaling in Living Breast Tumor Models"
Role: Principal Investigator
Agency: Department of Defense BCRP Type: Era of Hope Scholar Award W81XWH-05-1-0396
Period: 09/01/05-08/31/10.
The goal of this study is to investigate the signaling mechanism relating VEGFR2 activation to tumor vessel permeability, and to further develop the relevant noninvasive optical techniques.

"The Influence of Neuronal Activity on Breast Tumor Metastasis to the Brain"
Role: co-Principal Investigator
Agency: Department of Defense BCRP Type: Synergistic Idea Award BC060587
Period: 03/01/07-02/29/09
The goal of this study is to investigate the role that the extracellular matrix alterations induced by dendritic spine motility plays in breast tumor metastasis.

“Dynamic *in vivo* imaging and quantification of collagen microstructure and turnover in breast tumor models. “
Role: Principal Investigator
Agency: The Pew Foundation Type: Pew Scholar in the Biomedical Sciences Award
Period: 7/01/07-6/30/11
The goal of this study is to investigate collagen turnover in breast tumor models using novel microscopy techniques.

Completed Research Support:

Dates	Grant Number	P.I.	Type
1996-1999	NIH#T32-GM08267	Dr. Watt Webb	Molecular Biophysics Training Grant
1999-2000	NIH#T32-CA73479	Dr. Rakesh Jain	Integrative Pathophyisology of Tumors
2000-2002	NIH#F32-CA88490	Dr. Edward Brown	NRSA Postdoctoral Research Award
2000-2005	NIH#P01 CA80124	Dr. Rakesh Jain	NIH Program Project Grant
2000-2005	NIH#R24 CA85140	Dr. Rakesh Jain	Bioengineering Research Partnership
2003-2004	IRG-87-007-13	Dr. Edward Brown	American Cancer Society Grant
2003-2006	RG-05-0007	Dr. Edward Brown	Whitaker Biomedical Engineering Grant

Invited Lectures

"3D-Resolved Uncaging of Calcium Using Two-Photon Excitation." Invited lecture presented at Max Planck Institut fur Biophysikalische Chemie. Gottingen, Germany, 1997.

"Uncaging Using Two-Photon Microscopy." Invited lecture presented at Universitat des Saarlandes, Homburg, Germany, 1997.

"Quantitative Photochemical Applications of Multiphoton Laser-Scanning Microscopy." Invited lecture presented at Wake Forest University Dept. of Physics, Winston-Salem, NC, 1999.

"Quantitative Photochemical Applications of Multiphoton Laser-Scanning Microscopy." Invited lecture presented at Harvard University Dept. of Physics, Cambridge, MA, 1999.

"Quantitative Photochemical Applications of Multiphoton Laser Scanning Microscopy." and **"**In Vivo Measurement of Tumor Angiogenesis, Gene Expression, and Physiological Function Using the MPLSM" Invited lectures presented at Wellman Laboratory, MGH, Boston, MA, 2000.

"Measurement of physiological parameters in tumors in vivo using MPLSM." Invited lecture presented at the SPIE meeting on Progress in Biomedical Optics and Imaging, San Jose, CA, 2001. Published as: Brown E, Campbell R, Tsuzuki Y, Fukumura D, Jain RK. Measurement of physiological parameters in tumors in vivo using MPLSM. In: Periasamy A, So PTC, (eds). Progress in Biomedical Optics and Imaging. Proceedings of SPIE vol. 4262 Jan 21-23, Bellingham, Washington. SPIE; 2001 p. 134-146.

"Molecular Imaging of VEGF and HIF1 alpha." Invited lecture presented at the RCCA symposium, Dana-Farber Cancer Institute, Boston, MA, 2001.

"Quantitative Photochemical Applications of Multiphoton Laser-Scanning Microscopy." Invited lecture presented at the Renal Unit, MGH, Boston, MA, 2001.

"Microscopy of Living Tumors" Invited lecture presented at the CenSSIS Research and Industrial Collaboration Conference, Northeastern University, Boston, MA, 2002.

"Nonlinear Optical Microscopy of Tumors" Invited lecture presented at the Northeast Proton Center, Boston, MA, 2002.

"Dynamic Imaging of Collagen Content and Structure in Tumors Using Second Harmonic Generation." Short Talk presented at the SPIE meeting on Progress in Biomedical Optics and Imaging, San Jose, CA, 2003.

"Dynamic Imaging of Collagen in Tumors *in vivo* Using Second Harmonic Generation." Short Talk presented at the Keystone Symposium on Optical Imaging: Applications to Biology and Medicine, Taos, NM, 2003.

"Multiphoton Imaging of Tumor Biology and Angiogenesis" Invited lecture presented at the Department of Molecular Therapeutics, MD Anderson Cancer Center, Houston, TX, 2003

"Two Photon Imaging of Tumors" Invited lecture presented at the Department of Anatomy and Structural Biology, Albert Einstein College of Medicine, Bronx, NY, 2003

"Two Photon Imaging of Tumors" Invited lecture presented at the Department of Cell Biology, Yale University School of Medicine, New Haven, CT, 2003

"Two Photon Imaging of Tumors" Invited lecture presented at the Bioengineering Division, University of California-San Francisco, San Francisco, CA, 2003

"Two Photon Imaging of Tumors" Invited lecture presented at the Department of Radiation Oncology, University of Cincinnati, Cincinnati, OH, 2003

"Two Photon Imaging of Tumors" Invited lecture presented at the Department of Radiation Oncology, University of Michigan, Ann Arbor, MI, 2003

"Two Photon Imaging of Tumors" Invited lecture presented at the Department of Biochemistry and Biophysics, University of North Carolina, Chapel Hill, Chapel Hill, NC, 2003

"Two Photon Imaging of Tumors" Invited lecture presented at the Department of Radiology, University of Utah, Salt Lake City, UT 2003

"Tumor Pathophysiology Studied with the Multiphoton Laser-Scanning Microscope" Invited lecture presented at the Microscopy and Microanalysis Symposium: Advances in Quantitative Optical Microscopy, a Symposium in Honor of Watt Webb. San Antonio, TX, 2003.

"Diverse Imaging Processing Challenges in Radiation Oncology" Invited lecture presented at the Image Processing Mini-workshop, Massachusetts General Hospital, Boston, MA, 2004

"Multiphoton Imaging of Tumor Biology and Angiogenesis" Invited lecture presented at the Interdepartmental Program in Vascular Biology and Transplantation, Yale Medical School, New Haven, CT, 2004

"Can Antitumor Therapy be Improved with Multiphoton Laser-Scanning Microscopy?" Invited lecture presented at the Department of Biomedical Engineering, Yale University, New Haven, CT, 2004

"Nonlinear Optical Microscopy of Tumors" Invited lecture presented at the Biomedical Optical Spectroscopy, Imaging & Diagnostics Topical Meeting of the Optical Society of America. Miami, FL, 2004

"Can Antitumor Therapy be Improved with Multiphoton Laser-Scanning Microscopy?" Invited lecture presented at the Department of Cancer Biology, Vanderbilt University, Nashville, TN, 2004

"Can Antitumor Therapy be Improved with Multiphoton Laser-Scanning Microscopy?" Invited lecture presented at the International Institute of Molecular and Cellular Biology, Warsaw, Poland, 2004

"Can Antitumor Therapy be Improved with Multiphoton Laser-Scanning Microscopy?" Invited lecture presented at the Department of Bioengineering, PAN, Warsaw, Poland, 2004

"Can Antitumor Therapy be Improved with Multiphoton Laser-Scanning Microscopy?" Invited lecture presented at the Department of Biomedical Engineering, Cornell University, Ithaca, NY, 2004

"Multiphoton Imaging of Tumor Biology and Angiogenesis." Invited lecture presented at the Department of Biomedical Engineering, University of Rochester Medical Center, Rochester, NY, 2004

"Measurement of Diffusion Coefficients *in Vivo*: Why and How?" Invited lecture presented at the Department of Physics, Creighton University, Omaha, Nebraska, 2004

"Tumor Photobiology" Invited lecture presented at the First Annual Symposium on Modern Imaging and Biophysical Methods in Cell Biology and Neuroscience. Creighton University, Omaha, Nebraska, 2004

"Multiphoton Imaging of Tumor Pathopysiology" Invited lecture presented at the Center for Engineering in Medicine, Shriners Hospitals for Children, Boston, MA, 2004

“High Resolution Imaging of Tumor Biology and Treatment” Invited lecture presented at the Engineering Foundation’s Advances in Optics for Biotechnology, Medicine, and Surgery, Breckenridge, CO, 2005

“Nonlinear Microscopy of Living Tumors and Their Treatment” Invited lecture presented at the IEEE International Symposium on Biomedical Imaging, Arlington, VA, 2006

“Angiogenic Signaling in Living Breast Tumor Models” Invited lecture presented at the BCRP LINKS meeting, Baltimore, MD, 2006

“Multiphoton Laser-Scanning Microscopy of Tumor biology” Invited lecture presented at the Department of Physics, Ithaca College, Ithaca, NY, 2007

Selected Abstracts

Shear J, **Brown E**, Adams S, Tsien R, Webb W. Two-photon excited photorelease of caged calcium. Annual Meeting of the Biophysical Society. 1996.

Brown E, Ellis-Davies G, Webb W. Quantitative two-photon calcium uncaging. Annual Meeting of the Biophysical Society 1998.

Majewska A, **Brown E**, Yuste R. Mechanism of calcium decay kinetics in spines from hippocampal pyramidal neurons. Society for Neuroscience Abstracts, 1999.

Brown E, Pluen A, Compton C, Boucher Y, Jain RK. Measurement of diffusion coefficients of spontaneous human tumors. Annual Meeting of the American Association for Cancer Research, 2000.

Padera T, Kadambi A, Stoll B, di Tomaso E, Mouta-Carreira C, **Brown E**, Munn L, Jain RK. Multiphoton imaging of VEGF-C induced peri-tumor lymphatic hyperplasia. Gordon Research Conference on Angiogenesis and Microcirculation, 2001.

Brown E, Boucher Y, Jain RK. Measurement of diffusion coefficients in spontaneous human tumors. Annual Meeting of the American Association for Cancer Research, 2002.

Campbell R, **Brown E**, Izumi Y, Mazzola L, Torchilin V, Fukumura D, Munn L, Jain RK. Interactions of PEGylated cationic liposomes with tumor vessels in mice. Annual Meeting of the American Association for Cancer Research, 2002.

Brown E, Fukumura D, Munn L, Jain RK. Imaging the motion of host cells in tumors *in vivo* using intravital microscopy. Annual Meeting of the Molecular Imaging Society 2002.

Abdul-Karim M, Al-Kofahi O, **Brown E**, Jain RK, Al-Kofahi K, Turner J, Roysam B. Automated *in vivo* change analysis of tumor vasculature from two-photon confocal image time series. SPIE meeting on Progress in Biomedical Optics and Imaging, 2003.

Brown E, McKee T, Pluen A, Boucher Y, Jain RK. Dynamic imaging of collagen content and structure in tumors using second harmonic generation. International Society for Optical Engineering Meeting on Progress in Biomedical Optics and Imaging, 2003.

Brown E, McKee T, Pluen A, Boucher Y, Jain RK. Dynamic imaging of collagen in tumors *in vivo* using second harmonic generation. Keystone Symposium on Optical Imaging: Applications to Biology and Medicine, 2003.